Journal of Alloys and Compounds 509 (2011) 1314–1321

Contents lists available at ScienceDirect

Journal of Alloys and Compounds

journal homepage: www.elsevier.com/locate/jallcom

Effects of K_2O–Li_2O doping on surface and catalytic properties of Fe_2O_3/Cr_2O_3 system

Gamil A. El-Shobaky[a,*], Awad I. Ahmed[b], Hassan M.A. Hassan[c], Shaymaa E. El-Shafey[a]

[a] Physical Chemistry Department, National Research Center, Dokki, Cairo, Egypt
[b] Faculty of Science, Chemistry Department, Mansoura University, Mansoura, Egypt
[c] Faculty of Science, Chemistry Department, Suez Canal University, Suez, Egypt

ARTICLE INFO

Article history:
Received 24 March 2010
Received in revised form 5 October 2010
Accepted 7 October 2010
Available online 15 October 2010

Keywords:
Fe_2O_3/Cr_2O_3 catalyst
CO oxidation by O_2
K_2O
Li_2O-doping

ABSTRACT

The effects of K_2O and Li_2O-doping (0.5, 0.75 and 1.5 mol%) of Fe_2O_3/Cr_2O_3 system on its surface and the catalytic properties were investigated. Pure and differently doped solids were calcined in air at 400–600 °C. The formula of the un-doped calcined solid was $0.85Fe_2O_3{:}0.15Cr_2O_3$. The techniques employed were TGA, DTA, XRD, N_2 adsorption at −196 °C and catalytic oxidation of CO oxidation by O_2 at 200–300 °C. The results revealed that DTA curves of pure mixed solids consisted of one endothermic peak and two exothermic peaks. Pure and doped mixed solids calcined at 400 °C are amorphous in nature and turned to α-Fe_2O_3 upon heating at 500 and 600 °C. K_2O and Li_2O doping conducted at 500 or 600 °C modified the degree of crystallinity and crystallite size of all phases present which consisted of a mixture of nanocrystalline α- and γ-Fe_2O_3 together with K_2FeO_4 and $LiFe_5O_8$ phases. However, the heavily Li_2O-doped sample consisted only of $LiFe_5O_8$ phase. The specific surface area of the system investigated decreased to an extent proportional to the amount of K_2O and Li_2O added. On the other hand, the catalytic activity was found to increase by increasing the amount of K_2O and Li_2O added. The maximum increase in the catalytic activity, expressed as the reaction rate constant (k) measured at 200 °C, attained 30.8% and 26.5% for K_2O and Li_2O doping, respectively. The doping process did not modify the activation energy of the catalyzed reaction but rather increased the concentration of the active sites without changing their energetic nature.

1. Introduction

The catalytic activity and selectivity of a large variety of catalysts can be modified by various methods such as loading on a finely divided support [1–6], subjecting to ionizing radiations [7–15] and doping with certain foreign oxides [16–22]. The loading on suitable support material results in an increase in the concentration of catalytically active constituents via increasing their dispersity and hindering their grain growth. The ionizing radiations might also increase the number of active components by splitting them into small-sized particles besides modifying their acidic properties [12,13]. The doping with certain foreign oxides such as Li_2O, K_2O or ZnO hinders the metal oxide–support interactions thus increasing the stability of catalytically active constituents [16–23]. This treatment induced significant changes in the physicochemical characteristics of the treated solids such as the electrical, magnetic, textural and acidity features of the resulting solid catalysts. Nano-sized catalytic systems could be prepared by a variety of methods including sol–gel, co-precipitation, laser controlled deposition, wet impregnation and convenient microwave heating [24–27].

The catalytic oxidation of CO by O_2 can be used as a convenient test reaction for investigating the catalytic properties of various catalytic systems. The oxidation state of the catalytically active component is an important factor in determining the catalytic activity of such systems in which the active component can exist in different oxidation states [2,3].

Carbon monoxide, emitted from many industrial processes and transportation activities, is considered as an important class of air pollutions. Supported noble metals (Au, Pt, Pd and Ru) are efficient catalysts for CO oxidation [28–32]. Since the precious metals are relatively rare and expensive, some transition metal oxide catalysts have been used as active solids for CO oxidation by O_2 to avoid the high cost of the precious metals [33–40].

We have found, in our recent study that Cr_2O_3 acted as a catalyst stabilizer of Fe_2O_3/Cr_2O_3 system via hindering the grain growth of Fe_2O_3 crystallites [41].

In our last paper [41] the effects of chemical composition and calcinations temperature of pure Fe_2O_3/Cr_2O_3 system on its surface and catalytic properties have been investigated. The results

* Corresponding author. Tel.: +20237494265.
E-mail addresses: elshobaky@yhoo.com, gamil_elshobaky@yahoo.com (G.A. El-Shobaky).

0925-8388/$ – see front matter © 2010 Elsevier B.V. All rights reserved.
doi:10.1016/j.jallcom.2010.10.023

revealed that the increase in Cr_2O_3 content increased the specific surface area and catalytic activity.

The present work reports the results of a study on the influence of Li_2O and K_2O-doping on the surface and catalytic properties of Fe_2O_3/Cr_2O_3 system. The techniques employed were TGA, DTA, XRD, adsorption of N_2 at −196 °C besides catalytic oxidation of CO oxidation by O_2 at different temperatures between 200 and 300 °C.

2. Experimental

2.1. Materials

Ferric and chromic mixed hydroxides were prepared by using co-precipitation method. This process was carried out using an aqueous solution of ferric and chromic mixed nitrate solutions. This method was carried out at 50 °C with continuous vigorous stirring, until a pH of 8 was attained. Concentrated NH_4OH solution subjected to pubbling by a current of dry air free from CO_2 flowing at a rate of 20 ml/min was used as precipitating agent. Different amounts of $Fe(NO_3)_3{\cdot}9H_2O$ and $Cr(NO_3)_3{\cdot}9H_2O$ of analytical grade, supplied by BDH company, were used. The amounts of ferric and chromic mixed nitrates were calculated in a manner that Fe/Cr atomic ratio was 0.85/0.15. The molecular formula of the prepared calcined mixed solids was $0.85Fe_2O_3{:}0.15Cr_2O_3$. The carefully washed mixed hydroxides were dried at 120 °C and then were heated at 400, 500 and 600 °C for 4 h.

Three Li_2O-doped and three K_2O-doped samples were prepared using the Fe/Cr mixed hydroxide samples having Fe/Cr atomic ratio equals to 0.85:0.15. Known amounts of the mixed hydroxides were impregnated with calculated amounts of lithium or potassium nitrates dissolved in the least amount of distilled water sufficient to make pastes. The pastes were dried at 120 °C until constant weight then calcined in air at 400, 500 and 600 °C for 4 h. The dopant concentrations were 0.5, 0.75 and 1.5 mol% Li_2O or K_2O.

Pure mixed solids were designated as FeCr, while those doped with K_2O were $FeCrK_1$, $FeCrK_2$ and $FeCrK_3$ containing 0.5, 0.75 and 1.5 mol% respectively. Li_2O-doped solids were designated as $FeCrLi_1$, $FeCrLi_2$ and $FeCrLi_3$ including 0.5, 0.75 and 1.5 mol%, respectively.

2.2. Techniques

2.2.1. Thermal analysis

Thermo gravimetric and differential thermal analyses (TGA and DTA) of different prepared uncalcined solids were carried out with the aid of Thermo analyzer (D-50) Shimadzu, Japan. About 2 mg of each sample was heated at a rate of 10 °C/min in a stream of dry nitrogen flowing at a rate 20 ml/min. The thermally inert reference material was sintered alumina (α-Al_2O_3). The temperature was measured with the aid of Pt/Rh (10%) thermocouple.

2.2.2. X-ray diffraction (XRD) analysis of different mixed oxides

X-ray powder diffractograms of the samples calcined at 400, 500 and 600 °C were determined using a Bruker diffractometer (Bruker D8 advance target). The scanning rate was fixed at 8° in 2θ/min for phase identification and 0.8° in 2θ/min for line broadening profile analysis, respectively. The X-ray patterns were recorded using Cu Kα1 with secondly monochromator (λ = 0.1545 nm), operated at 40 kV and 40 mA. The crystallite size was calculated from the line broadening profile analysis of the main diffraction lines of the phases present using the Scherrer equation [42].

$$D = \frac{K\lambda}{\beta_{1/2}\cos\theta}$$

where D is the mean crystallite diameter in Å, λ is the wave length of X-ray beam, K is the Scherrer constant (0.89), $\beta_{1/2}$ is the full-width at half-maximum (FWHM) of the main diffraction peak of crystalline phases and θ is the diffraction angle.

2.2.3. Measurements of different surface characteristics

The different surface characteristics of various solids were determined from analysis of nitrogen adsorption isotherms, carried out at −196 °C over various adsorbents. These characteristics include specific surface areas (S_{BET}), total pore volume (V_p), mean pore radius (r^-) and pore volume distribution ($\Delta v/\Delta r$). The different adsorption desorption isotherms were measured using Quantachrome NOVA Automated Gas sorbometer. The S_{BET} values were determined from linear portion of the BET equation. Another series of specific surface area (S_t) was determined from $V_l - t$ plots constructed using suitable standard t-curves depending on the values of the BET-C constant.

The values of V_p were computed from the relation $V_p = 15.45 \times 10^{-4} \times V_{st}$ cm^3/g, where V_{st} is the volume of nitrogen adsorbed at P/P^0 tends to unity. The values of r^- were determined from the equation

$$r^-(\text{Å}) = \frac{2V_p}{S_{BET}} \times 10^4$$

2.2.4. Apparatus for measuring the catalytic activity

Catalytic oxidation of CO by O_2 over the various catalysts was carried out at temperatures in the range of 200–300 °C using a static method. A stoichiometric mixture of CO and O_2 ($CO + 1/2O_2$) at a pressure of 2 Torr was used. A fresh catalyst sample (200 mg) was employed for each kinetic experiment and was activated by heating under a reduced pressure of 10^{-6} Torr for 1 h at 250 °C. The CO_2 produced was removed from the reaction system by freezing in a liquid nitrogen trap. The kinetics of the catalytic reaction was monitored by measuring the pressure of the reacting gases, using mercurury Mc Leod gauge, at different time intervals until no change in pressure was attained. This indicates that no further interaction between CO and O_2 occurs. The % decrease in pressure at a given time determines the percentage conversion of the catalytic reaction at that time. The saturation vapour pressure of CO at −196 °C being 160 Torr makes its liquefaction at that pressure improbable under the employed conditions (2 Torr) as shown by El-Shobaky et al. [43].

3. Results and discussion

3.1. Thermal analyses of different prepared mixed hydroxides

TGA and DTA curves of pure and doped un-calcined mixed solids were determined. The obtained TGA curves consists of four weight losses most of which took place at temperatures blew 500 °C. The thermal decomposition of ferric and chromic mixed hydroxides proceeds according to:

$$0.85Fe_2O_3 + 0.3Cr(OH)_3 \rightarrow 0.85Fe_2O_3 + 0.15Cr_2O_3 + 0.85x{\cdot}H_2O + 0.45H_2O$$

The value of x was readily determined in terms of the total weight lossobserved. The DTA curves of the un-calcined pure mixed solid consist of two exothermic peaks and an endothermic one with their maxima at temperature near from each other for the variously investigated solids. The amounts of dopant nitrates (lithium and potassium) added were very small. Their thermal decomposition did not exert any detectable influence in TGA and DTA curves of the doped solids.

Figs. 1 and 2, respectively, depict the TGA and DTA curves of FeCr, $FeCrK_3$ and $FeCrLi_3$ samples. The TGA curve of FeCr sample is composed of four distinct weight loss processes. The first process extends between 27and 138 °C, the second from 138 to 271 °C, the third from 271 to 453 °C and the fourth from 454 to 570 °C. These processes are followed by weight losses of 12.76, 12.4, 2.05 and 1.2%, respectively. So, the total weight loss of FeCr solid sample is 28%. This value might suggest the formula of hydrated ferric oxide in the doped sample to be $Fe_2O_3{\cdot}3.5H_2O$. The DTA curve of this sample (pure one) consists of three peaks. The first peak is endothermic relatively sharp and strong, the second peak is exothermic strong and sharp, and the third peak is exothermic broad and weak. The maxima of these peaks are located at 89.8, 198.23 and 619.78 °C. The first two peaks correspond to removal of physisorbed water, water of constitution of hydrated ferric oxide and dehydroxylation of chromic oxide yielding ferric oxide and chromic oxide, respectively. The third peak might correspond to crystallization of ferric oxide into α-Fe_2O_3 phase.

The TGA curve of $FeCrK_3$ sample is composed of four distinct weight loss processes. The first process extends between 34 and 149 °C, the second from 150 to 329 °C, the third from 437 to 585 °C and the fourth from 586 to 773 °C. These processes are followed by weight losses of 2.51, 7.87, 5.2 and 18.95%, respectively. So the total weight loss of $FeCrK_3$ solid sample is 34.2%. This value might suggest the formula of hydrated ferric oxide in the doped sample to be $Fe_2O_3{\cdot}4H_2O$. The DTA curve of this sample consists of seven endothermic peaks and one exothermic. These peaks vary between weak and strong and being broad and sharp. The last peak is exothermic peak, strong and sharp. The maxima of these peaks are located at 71.46, 140.9, 245.8, 278.8, 331.6, 707.8, 797.3 and 884.1 °C. The first five peaks correspond to removal of physisorbed water, water of constitution of hydrated ferric oxide and dehydrox-

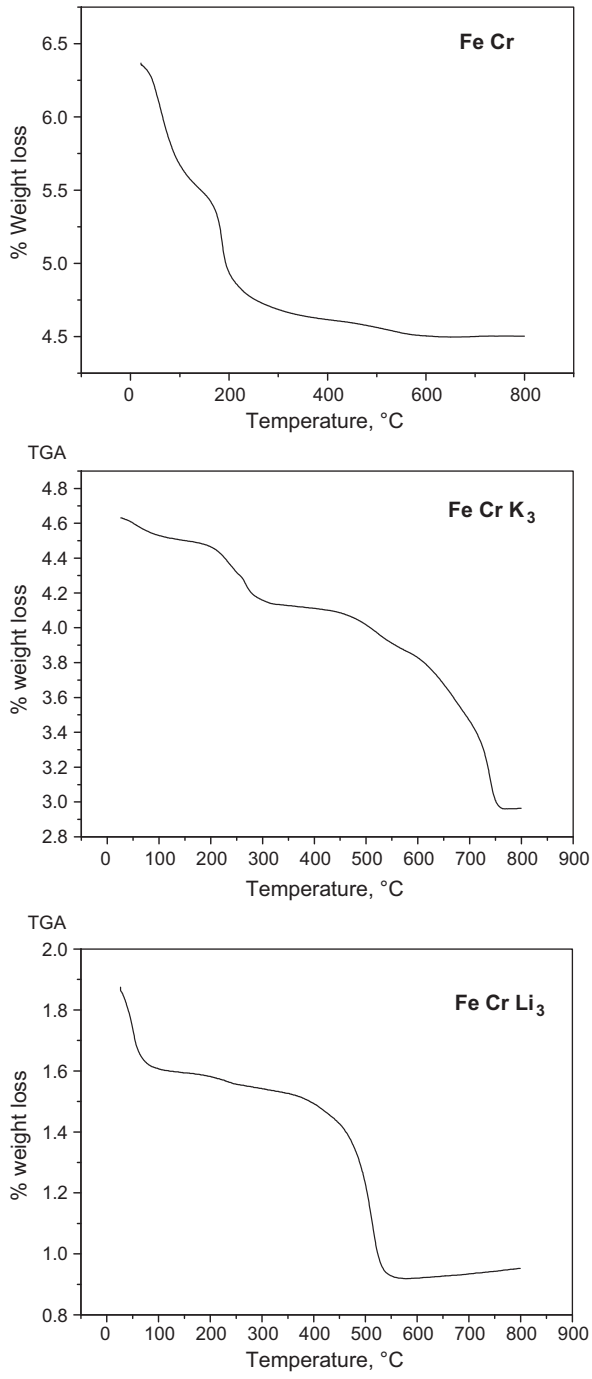

Fig. 1. TGA curves of un-calcined FeCr, $FeCrK_3$ and $FeCrLi_3$.

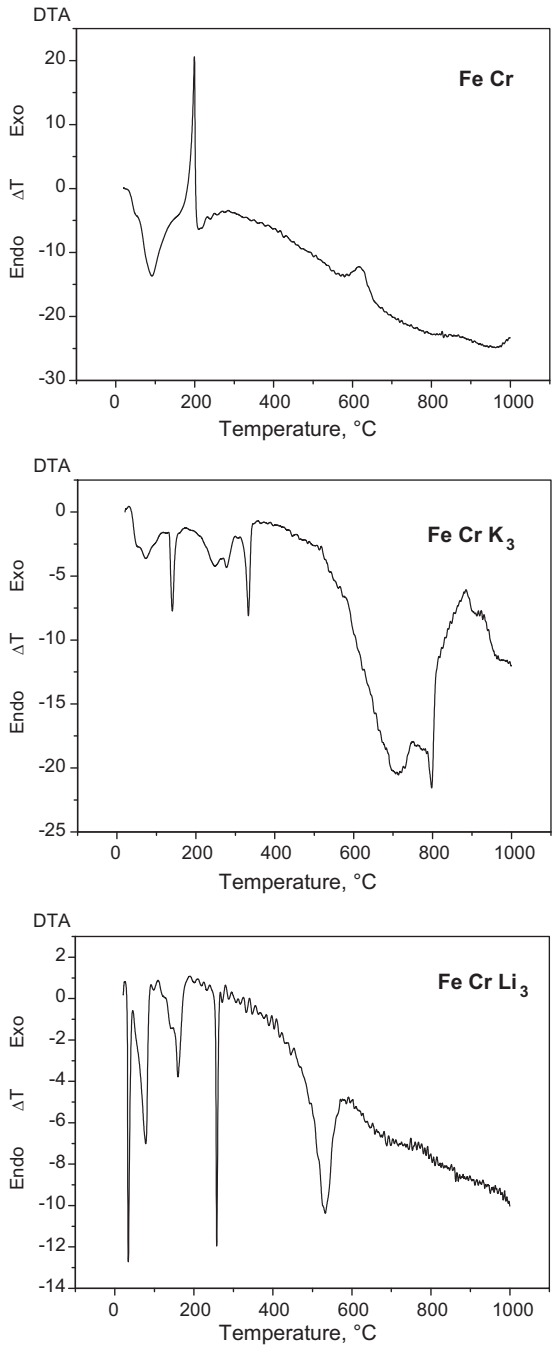

Fig. 2. DTA curves of un-calcined FeCr, $FeCrK_3$ and $FeCrLi_3$ solids.

ylation of chromic oxide yielding ferric oxide and chromic oxide, respectively. The last two peaks might correspond to crystallization of ferric oxide into α- and γ-Fe_2O_3 and also the possible formation of potassium ferrite. The crystallization of Fe_2O_3 into α- and γ-phases and the possible formation of the ferrite phase was confirmed latter by XRD investigation, as it is discussed in the next section.

The TGA curve of the heavily Li_2O-doped sample consisted of three distinct weight loss processes. The first process extends between 30 and 110 °C, the second from 111 to 394 °C and the third from 395 to 577 °C. These processes are followed by weight losses of 12.77, 0.9 and 30.7%, respectively. So, the total weight loss of $FeCrLi_3$ solid sample is 43.1%. This value might suggest the formula of hydrated ferric oxide in the doped sample to be $Fe_2O_3{\cdot}7H_2O$. The DTA curve of this sample consists of five endothermic peaks. All peaks are strong and sharp. The maxima of these peaks are located at 33.3, 77.25, 159.05, 257.89 and 530.62 °C. The first four peaks correspond to removal of physisorbed water, water of constitution of hydrated ferric oxide and dehydroxylation of chromic oxide yielding ferric oxide and chromic oxide, respectively. The last peak might correspond to crystallization of ferric oxide into α- and γ-phases. The absence of any peak for the possible formation of lithium ferrite might be attributed to the very slow rate of formation of this compound that could not be easily detected by DTA measurements.

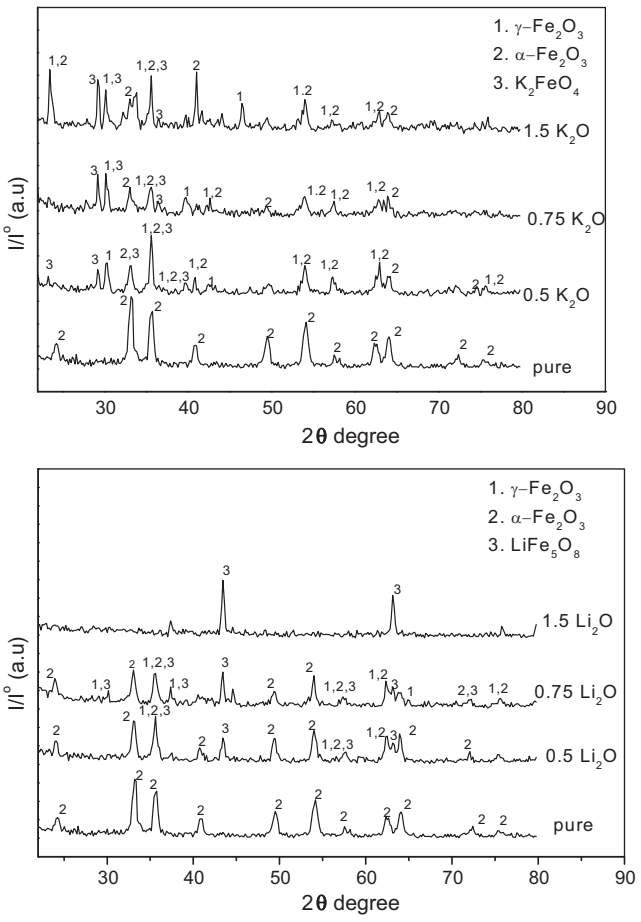

Fig. 3. X-ray diffractograms of pure and 0.5, 0.75 and 1.5 mol%. K_2O and Li_2O-doped samples calcined at 500 °C

3.2. XRD investigation of pure and variously doped solids

The XRD diffractograms of pure and variously doped solids heated at 400, 500 and 600 °C were determined. Fig. 3 shows representative X-ray diffractograms of different investigated solids calcined at 500 °C. Pure and variously doped solids calcined at 400 °C were amorphous in nature. Examination of Fig. 3 shows the following: (i) Pure solids crystallized into α-Fe_2O_3 upon heating at 500 or 600 °C. (ii) K_2O-doping (0.5–1.5 mol%) conducted at 500 or 600 °C led to the appearance of γ-Fe_2O_3 as a major phase together with α-Fe_2O_3 and new diffraction lines at d = 2.97 Å and 2.94 Å corresponding to K_2FeO_4, JCPDS-ICDD 25-652. (iii) Li_2O-doping (0.5 or 0.75 mol%) conducted at 500 or 600 °C led to the appearance of γ-Fe_2O_3 as a major phase besides α-Fe_2O_3 and new diffraction lines at d = 1.47 Å and 2.08 Å which correspond to $LiFe_5O_8$ [44]. (iv) Increasing the dopant concentration to 1.5 mol% Li_2O led to the complete disappearance of all ferric oxide phases and $LiFe_5O_8$ was only the detected phase present.

The fact that the amount of Li_2O added is far below the detection limit of X-ray diffractometer points out to the enriched presence of the dopant agent in the top surface layers of doped solids. The enriched presence of Li_2O-dopant on top surface layers of doped solids had been reported by El-Shobaky et al. [45] in different doped catalytic systems prepared by wet impregnation method. The disappearance of ferric oxide phases could be tentatively attributed to the solid–solid interaction between Li_2O and all surface ferric oxides.

It is known that the crystal of γ-Fe_2O_3 generally possess an imperfect cubic spinel structure, which is different from that of α-Fe_2O_3, hexagonal structure. The imperfect spinel of γ-Fe_2O_3 allows promoter such as Cr to be incorporated into vacant sites in the γ-Fe_2O_3 resulting in less sintering of active phase in the catalysts consisting of γ-Fe_2O_3 than those containing α-Fe_2O_3 under identical operating conditions [46]. The crystallite size and degree of crystallinity of different crystalline phases in pure and doped solids calcined at various temperatures are given in Tables 1 and 2. It is clearly shown from these tables that K_2O and Li_2O-doping (0.5–1.5 mol%) conducted at 500 or 600 °C increased the degree of crystallinity and crystallite size of phase present which consisted of a mixture of α- and γ-Fe_2O_3 together with K_2FeO_4 and $LiFe_5O_8$ phases (JCPDS-ICDD 25-652 [44]).

The formation of potassium and lithium ferrites took place according to:

$$Fe_2O_3 + 2K_2O + 3/2O_2 \rightarrow 2K_2FeO_4$$

$$5Fe_2O_3 + Li_2O \rightarrow 2LiFe_5O_8$$

The crystallization of ferric oxide into α- and γ-Fe_2O_3 together with the formation of K_2FeO_4 and $LiFe_5O_8$ phases are expected to modify the surface characteristics of pure and variously doped solids calcined at 400–600 °C.

3.3. Surface properties of pure and doped solids

The V_l–t plots (not given) of the investigated solids calcined at 500 °C showed an upward deviation, suggesting the domination of wide pores. The value of r^- varies between 20 and 83 Å depending on nature of dopant and its concentration. So, all adsorbents are considered as mesoporous solids. However, one can not overlook the possible existence of a small portion of macropores.

The slopes of all V_l–t plots constructed for the investigated solids enable the S_t to be determined. The computed S_t values are given in Table 3.

The pore volume distribution curves ($\Delta v/\Delta r$) for pure and heavily doped adsorbents calcined at 500 °C were determined. The curves obtained are illustrated in Fig. 4. These curves show multimodal distribution for pores present in pure and Li_2O-doped adsorbents. The maxima of the most probable pore radius are located at 18, 29 and 46 Å for pure solid calcined at 500 °C and at 15, 18 and 54 Å for 1.5 mol%-doped solid calcined at the same temperature. However, the majority of pores present in the doped adsorbent measured pore radius between 15 and 18 Å. On the other hand ($\Delta v/\Delta r$), curve of adsorbent doped with 1.5 mol% K_2O shows unimodal distribution of pores with a maximum present at a value of 36 Å. These findings might suggest that K_2O-doping led to the widening of pores present. K_2O-doping shifted the value of most probable pore radius from 18, 29 Å to 36 Å. The comparison between the areas of ($\Delta v/\Delta r$) curves shows that the doping process conducted at 500 °C decreased the volume of pores present. The decrease was, however, more pronounced in case of Li_2O-doping. These results agree well with the V_p values measured for pure and doped solids calcined at 500 °C (cf. Table 3). Examination of Table 3 reveals the following: (i) The values of S_{BET} and S_t for all adsorbents investigated are close to each other which justifies the correct choice of standard t-curve used in pore analysis and indicates the absence of the ultra micro pores. (ii) K_2O-doping followed by calcination at 500 °C resulted in a progressive decrease in the S_{BET} of the treated solids reaching to about 29% for the heavily doped samples. (iii) Treatment of the investigated system with 0.5 and 0.75 mol% of Li_2O followed by calcination at 500 °C led to a measurable increase in its S_{BET} of about 17% and 98%, respectively. On the other hand, the addition of 1.5 mol% Li_2O brought about a sudden drop (about 85%) in the S_{BET} of the treated solids. This drop could be tentatively

Table 1
XRD data of pure Fe_2O_3–Cr_2O_3 and variously K_2O-doped solids calcined at 400–600 °C.

Catalyst	Calcination temperature (°C)	Phases present	Crystallite size (nm)	Degree of crystallinity (a.u.)[a]
FeCr	400	Amorphous	–	–
	500	α-Fe_2O_3	22	12
	600	α-Fe_2O_3	35	26
$FeCrK_1$	400	Amorphous	–	–
	500	γ-Fe_2O_3	37	16
		K_2FeO_4	34	8
		α-Fe_2O_3	25	7
	600	γ -Fe_2O_3	52	31
		α-Fe_2O_3	32	18
		K_2FeO_4	31	15
$FeCrK_2$	400	Amorphous	–	–
	500	K_2FeO_4	69	11
		γ-Fe_2O_3	39	7
		α-Fe_2O_3	42	8
	600	γ-Fe_2O_3	46	15
		K_2FeO_4	54	11
		α-Fe_2O_3	29	10
$FeCrK_3$	400	Amorphous	–	–
	500	γ-Fe_2O_3	40	13
		K_2FeO_4	64	12
		α-Fe_2O_3	15	8
	600	K_2FeO_4	79	19
		γ-Fe_2O_3	64	17
		α-Fe_2O_3	38	15

[a] The peak area of the main diffraction lines of α- and γ-Fe_2O_3 was taken as a measure of degree of crystallinity of these phases.

attributed to the presence of some of Li_2O added in the pores, causing an effective blocking of these pores and hence decreasing its specific surface area.

The observed increase in the S_{BET} for Fe_2O_3/Cr_2O_3 system due to doping with Li_2O (0.5 and 075 mol%) could be attributed to the narrowing of pores (r^- decreases from 83 to 20 Å) in the doped solids. Also, the observed increase in the S_{BET} could be attributed to the creation of new pores during the thermal treatment of the doped solids via liberation nitrogen oxides gases during thermal decomposition of $LiNO_3$ dopant added. Similar results have been reported in the case of CuO/Al_2O_3 [47], $CuO–ZnO/Al_2O_3$ [48] Cr_2O_3/Al_2O_3 [49] and NiO/Al_2O_3 systems [50,51].

The limited decrease in the S_{BET} for Fe_2O_3/Cr_2O_3 system due to doping with K_2O could be attributed to a possible blockage of the pores by K_2O. The decease in surface area might be also attributed to the formation of potassium ferrite. The formation of this compound

Table 2
XRD data of pure Fe_2O_3–Cr_2O_3 and variously Li_2O-doped solids calcined at 400–600 °C.

Catalyst	Calcination temperature (°C)	Phases present	Crystallite size (nm)	Degree of crystallinity (a.u.)[a]
FeCr	400	Amorphous	–	–
	500	α-Fe_2O_3	22	12
	600	α-Fe_2O_3	35	26
$FeCrLi_1$	400	Amorphous	–	–
	500	γ-Fe_2O_3	39	13
		α-Fe_2O_3	31	12
		$LiFe_5O_8$	50	6
	600	γ-Fe_2O_3	65	30
		$LiFe_5O_8$	48	19
$FeCrLi_2$	40	Amorphous	–	–
	500	γ-Fe_2O_3	29	12
		$LiFe_5O_8$	63	11
		α-Fe_2O_3	24	10
	600	γ-Fe_2O_3	31	18
		$LiFe_5O_8$	50	15
$FeCrLi_3$	400	Amorphous	–	–
	500	$LiFe_5O_8$	53	16
	600	$LiFe_5O_8$	87	15

[a] The peak area of the main diffraction lines of α- and γ-Fe_2O_3 was taken as a measure of degree of crystallinity of these phases.

Table 3
Some surface characteristics of pure and K_2O-or Li_2O-doped Fe_2O_3/Cr_2O_3 solids calcined at 500 °C.

Adsorbent	S_{BET} (m^2/g)	S_t (m^2/g)	Total pore volume, V_p (cm^3/g)	Mean pore radius, r^- (Å)	BET-C constant
FeCr	52	54	0.21658	83	152
$FeCrK_1$	37	35	0.0555	30	3
$FeCrK_2$	35	32	0.03697	21	3
$FeCrK_3$	37	33	0.03635	20	3
$FeCrLi_1$	61	58	0.1106	36	5
$FeCrLi_2$	103	99	0.16243	32	4
$FeCrLi_3$	7.4	7.2	0.0242	65	−9

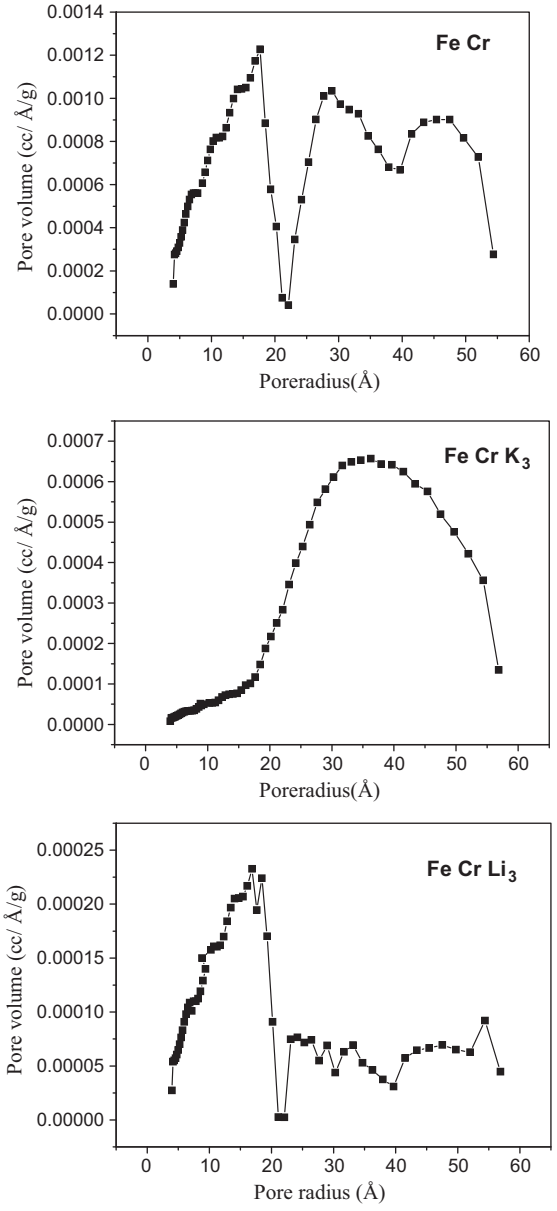

Fig. 4. Pore volume distribution curves of FeCr, $FeCrK_3$ and $FeCrLi_3$ samples calcined at 500 °C.

is normally accompanied by a significant loss in their porosity [52], followed by a corresponding decrease in their S_{BET} values.

The observed changes in the surface characteristics of the investigated system due to doping with K_2O and Li_2O could induce possible changes in its catalytic activity.

3.4. Catalytic activity of pure and doped solids

The oxidation of CO by O_2 was carried out at different temperatures within 200 and 300 °C over pure and variously doped solids calcined at 500 °C. First order kinetics was observed in all cases; the slopes of the first order plots determine the values of reaction rate constant (k) measured at a given temperature over a given catalyst sample. Fig. 5 shows representative first order-plots of CO oxidation by O_2 carried out at 200, 250, and 300 °C over FeCr, $FeCrK_3$ and $FeCrLi_3$ solids. The k values were calculated for different solids are given in Table 4. Examination of Table 4 shows the following: k increases progressively upon increasing the Li_2O or K_2O contents in the doped solids. The maximum increase in the k_{200} °C value is

Table 4
Reaction rate constant per unit mass ($k \times 10^{-3}$ min^{-1} g^{-1}) and Activation energy ΔE_a for the catalytic oxidation of CO by O_2 over Fe_2O_3/Cr_2O_3 system being doped by different amounts of Li_2O or K_2O and calcined at 500 °C.

Catalyst	Reaction temperature (°C)	k (10^{-3} min^{-1} g^{-1})	ΔE_a (kJ/mol)
FeCr	200	7.8	2.7
	250	8.1	
	300	8.9	
$FeCrK_1$	200	9	3.3
	250	10	
	300	11	
$FeCrK_2$	200	9.6	3.7
	250	11.1	
	300	11.2	
$FeCrK_3$	200	10.2	2.7
	250	10.8	
	300	11.5	
$FeCrLi_1$	200	8.8	3.0
	250	9.3	
	300	10.1	
$FeCrLi_2$	200	9.1	4.0
	250	9.7	
	300	10.9	
$FeCrLi_3$	200	9.9	1.0
	250	10.1	
	300	10.4	

due to doping with 1.5 mol% K_2O or 1.5 mol% Li_2O for the reaction carried out at 200 °C attained 30.8% and 26.5%, respectively. These results clearly indicate the role of nature of dopant in modifying the catalytic activity in CO oxidation by O_2.

The parameters, which determine the catalytic activity of Fe_2O_3/Cr_2O_3 system, include the concentration of catalytically active constituents on the top surface layers of treated solids and their interaction. The doping process might change the number of active sites on the catalyst's surface contributing in chemisorption and catalysis of CO-oxidation by O_2. The energetic nature of these sites could also be influenced by doping. Furthermore, the mechanism of the catalytic reaction could be changed by doping.

The change in the catalytic activity of the system investigated due to doping either with K_2O or Li_2O could be discussed in terms of the following parameters: (i) the change in S_{BET}, (ii) the change in the crystallite size of the catalytic reactive constituents (some of surface Fe_2O_3), (iii) conversion of some of α-Fe_2O_3 into γ-Fe_2O_3, (iv) conversion of some of Fe_2O_3 into lithium or potassium ferrites. The increase in the S_{BET} is normally accompanied by an increase in the activity. The decrease in the crystallite size of Fe_2O_3 might also be followed by an increase in the catalytic activity and vice versa. It is well known that γ-Fe_2O_3 is more active than α-Fe_2O_3 [46]. So, the conversion of some of α-Fe_2O_3 to γ-Fe_2O_3 should be expected to increase the catalytic activity of the treated catalyst. The formation of lithium or potassium ferrites (devoted with smaller activity compared to Fe_2O_3) might decrease the catalytic activity of the doped solids. In order to account for the induced change in the S_{BET}, the reaction rate constant per unit surface area (k^-) was calculated and the computed values for the reaction carried out at 200 °C were 15×10^{-5}, 24.3×10^{-5}, 27.4×10^{-5} and 27.6×10^{-5} min^{-1}m^{-2} for pure sample and those doped with 0.5, 0.75 and 1.5 mol% K_2O, respectively. These values attained 14.4×10^{-5}, 8.8×0^{-5} and 133.8×10^{-5} min^{-1}m^{-2} for 0.5, 0.75 and 1.5 Li_2O-doped solids, respectively.

The fact that the calculated values of k −200 °C are different from each other may indicate that the doping process increased the catalytic activity of the investigated system. The increase was, however, more pronounced in the case of K_2O-doping. Furthermore, the induced changes in the specific surface area due to doping are not a dominant parameter determining the catalytic activity of the system investigated. The formation of lithium and potassium ferrites in the doped solids might decrease their catalytic activity. This

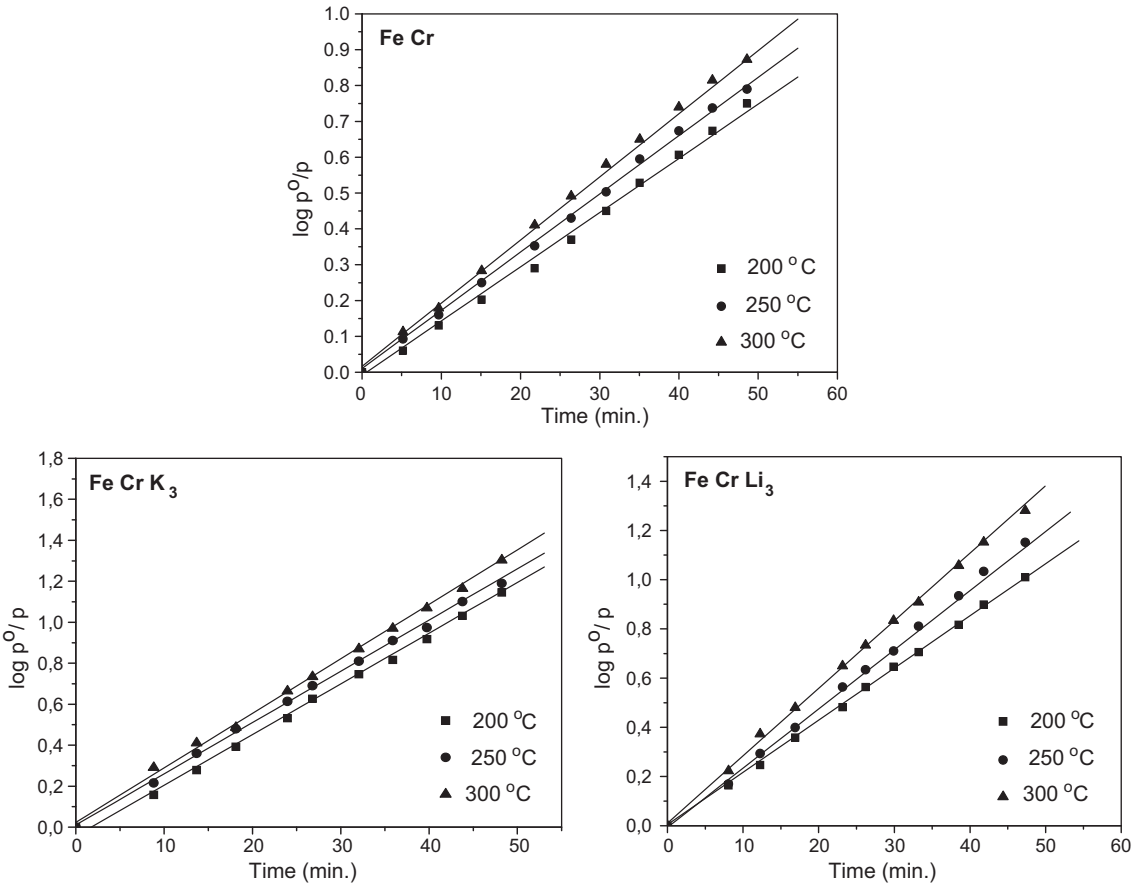

Fig. 5. First order-plots of CO oxidation by O_2 carried out at different temperatures over FeCr, $FeCrK_3$ and $FeCrLi_3$ systems calcined at 500 °C.

expectation was not verified experimentally since an increase and not decrease in the activity was found. So, the observed increase in the catalytic activity due to doping could be, mainly, attributed to the role of the dopant used in increasing the thermal stability of γ-Fe_2O_3 phase.

3.5. Effects of Li_2O and K_2O doping on ΔE of the catalyzed reaction

Determination of the apparent activation energy (ΔE) of the investigated catalytic reaction sheds some light on the possible change in the mechanism of the catalyzed reaction. Furthermore, it may give useful information about the possible alteration in the concentration and nature of catalytically-active constituents.

The values of k measured at temperatures varying between 200 and 300 °C over the variously doped solids enable the estimation of ΔE value by direct application of the Arrhenius equation. Table 5 lists the estimated values of ΔE and the values of the pre-exponential factor (A) of the Arrhenius equation. Table 5 shows that A changes with doping, which may be an indication of the heterogeneity of the catalyst surface. In addition, it shows that ΔE and ln A values fluctuate in the same manner, indicating that the changes in ΔE values come from a corresponding changes in ln A values. This speculation could be confirmed from recalculation of ΔE values for the reaction conducted over pure and variously doped solids. This calculation was done via adopting the ln A value for pure sample to all doped samples calcined at the same temperature. The recalculated values of the activation energies (ΔE^*) are given in Table 5. ΔE^* values of pure and doped solids showed almost the same values (2.85 ± 0.15 kJ/mol). This finding suggested clearly that doping Fe_2O_3/Cr_2O_3 system either with Li_2O or K_2O followed by heating at 500 °C, did not much modify the activation energy of the catalytic reaction. The doping process may change the concentration of active sites involved in the catalyzed reaction.

Table 5
Computed activation energies (ΔE, ΔE^*) and logarithm of pre-exponential factor of the Arrhenius equation for the catalytic reaction carried out over pure Fe_2O_3/Cr_2O_3 system being doped by different amounts of Li_2O or K_2O and calcined at 500 °C.

Catalyst	ΔE (kJ/mol)	ΔE^* (kJ/mol)	ln A
FeCr	2.7	2.7	−1.88
$FeCrK_1$	3.34	2.8	−1.54
$FeCrK_2$	3.7	2.9	−1.43
$FeCrK_3$	2.7	2.9	−1.58
$FeCrLi_1$	3.0	3.0	−1.67
$FeCrLi_2$	4.0	2.7	−1.38
$FeCrLi_3$	1.0	2.7	−2.04

4. Conclusions

The following points are the main conclusions of this study:

1. Pure and doped solids, calcined at 400 °C, are amorphous in nature. Pure mixed solids crystallized into α-Fe_2O_3 upon heating at 500 or 600 °C. On the other hand, the addition of K_2O or Li_2O-doping (0.5–1.5 mol%), followed by heating at 500 or 600 °C, led to the formation of α- and γ-Fe_2O_3 phases together with K_2FeO_4 and $LiFe_5O_8$ phases.
2. Doping with 1.5 mol% Li_2O, followed by calcination at 500 or 600 °C led to the complete disappearance of all ferric oxide phases.

3. Doping either with K_2O or Li_2O, followed by calcination at 500 °C brought about significant changes in its surface characteristics. K_2O-doping decreases both the S_{BET} and V_p due to an effective increase in the *r*-value. On the other hand, Li_2O doping exerted opposite effects.
4. The catalytic activity, expressed as $k_{200\,^\circ C}$, was found to increase by increasing the amounts of dopant added. The maximum increase due to doping with 1.5 mol% K_2O or 1.5 mol% Li_2O attained 30.8% and 26.5%, respectively.
5. The increase in the catalytic activity, expressed as the reaction rate constant per unit surface area measured at 200 °C, $k_{-200\,^\circ C}$, due to doping either with K_2O or Li_2O was much more pronounced as compared to that calculated for $k_{200\,^\circ C}$ values.
6. The estimated values of activation energy of catalytic reaction were relatively small, indicating the big catalytic activity of the investigated solids. Li_2O and K_2O dopant did not modify the mechanism of catalytic oxidation of CO by O_2, carried out at 200–300 °C over various solids. It rather changed the concentration of catalytically active constituents (surface Fe_2O_3 crystallites) without modifying their energetic nature.

References

[1] S. Colussi, C. de Leitenburg, A. Trovarelli, J. Alloys Compd. 374 (2004) 387–392.
[2] L Zhang, M.M. Jean-Marc, U.S. Ozkan, Appl. Catal. A: Gen. 357 (2009) 66–72.
[3] G.A. El-Shobaky, G.A. Fagal, T.M.H. Saber, Bull. Soc. Chim. Fr. 4 (1987) 551.
[4] J.H.A. Martens, R. Prins, Appl. Catal. 46 (1989) 31.
[5] C.L. ÓYoung, J. Phys. Chem. 93 (1989) 2016.
[6] G.A. El-Shobaky, Th El-Nabarawy, G.A. Fagal, A.S. Ahmed, Mater. Lett. 31 (1993) 3291.
[7] K.K. Kuzemaev, G.T. Tugelbaeva, Trans. Inst. Org. Katal. Elektrokhim. Akad. Nauk. Kaz. SSR 20 (1980) 53.
[8] K.K. Kuzembaev, Zh. Fiz. Khim. 54 (1980) 53.
[9] G.A. El-Shobaky, M.M. Doheim, A.M. Ghozza, Radiat. Phys. Chem. 69 (2004) 31–37.
[10] H.G. El-Shobaky, W.M. Shaheen, Radiat, Phys. Chem. 66 (2003) 55–65.
[11] G.A. El-Shobaky, G.A. Fagal, N. Petro, A.M. Dessouki, Radiat. Phys. Chem. 29 (1987) 39.
[12] G.A. El-Shobaky, N.H. Amin, G.A. Fagaal, J. Radioanal. Nucl. Chem. Art. 177 (12) (1994) 211.
[13] G.A. El-Shobaky, A.S. Ahmad, M. Mokhtar, J. Radioanal. Nucl. Chem. Art. 219 (1) (1997) 89.
[14] V. Mcka, V. Tabacik, Radiat. Phys. Chem. 38 (1991) 285.
[15] G.A. El-Shobaky, G.A. Fagal, H.G. El-Shobaky, S.M. El-Khouly, Colloids Surf. A 152 (1999) 275.
[16] M. Gabás, J.-R. Ramos-Barrado, A. Jiménez-López, E. Rodríguez-Castellón, J. Mérida-Robles, J. Alloys Compd. 317 (2001) 153–159.
[17] R. Kam, C. Selomulya, R. Amal, J. Scott, J. Catal. 273 (2010) 73–81.
[18] G.A. El-Shobaky, Th. El-Nabarawy, G.A. Fagal, J. Serb. Chem. Soc. 55 (1990) 21.
[19] G.A. El-Shobaky, A.N. Al-Noaimi, A. Abdeel-Aal, A.M. Ghozza, Mater. Lett. 22 (1995) 167.
[20] G.A. El-Shobaky, G.A. Fagal, M. Mokhtar, Appl. Catal. A 155 (1997) 167.
[21] G.A. El-Shobaky, G.A. Fagal, A.M. Ghozza, M. Mokhtar, Colloids Surf. A 142 (1998) 17.
[22] G.A. El-Shobaky, A.M. Ghozza, H.G. El-Shobaky, Adsorpt. Sci. Technol. 16 (6) (1998) 415.
[23] P.H. Bolt, M.E. Van Ipenburg, J.W. Geus, F.H.M. Habraken, Mater. Res. Symp. Proc. 344 (1994) 15.
[24] G.A. El-Shobaky, A.M. Turky, N.Y. Mostafa, S.K. Mohamed, J. Alloys Compd. 493 (2010) 415–422.
[25] S. Abd El All, G.A. El-Shobaky, J. Alloys Compd. 479 (2009) 91–96.
[26] R. Vijay, R. Sundaresan, M.P. Maiya, S.S. Murthy, J. Alloys Compd. 424 (2006) 289–293.
[27] G.A. El-Shobaky, M.M. Dohiem, S.A. Esmail, H.A. El-Boohy, A.M. Ahmed, J. Radioanal. Nucl. Chem. Art. 275 (2008) 487–495.
[28] A.M. Ibrahim, M.M. Abd El-Latif, M.M. Mahmoud, J. Alloys Compd. 506 (2010) 201–204.
[29] M. Harute, S. Isubota, T. Kobayshi, H. Kageyama, M.J. Genet, B. Delmon, J. Catal. 144 (1993) 175.
[30] A. De Sarkar, B.C. Khanra, J. Mol. Catal. A: Chem. 229 (2005) 25.
[31] A.K. Santra, D.W. Goodman, Electrochim. Acta 47 (2002) 3595.
[32] A.M. Visco, A. Donato, C. Milone, S. Galvagno, React. Kinet. Catal. Lett. 61 (1997) 219.
[33] S. Minicò, S. Scirè, C. Crisafulli, A.M. Visco, S. Galvagno, Catal. Lett. 47 (1997) 273.
[34] G. Marbán, A.B. Fuertes, Appl. Catal. B: Environ. 57 (2005) 43.
[35] G.A. El-Shobaky, A.M. Ghozza, Mater. Lett. 58 (2004) 699.
[36] X. Zheng, S. Wang, S. Wang, S. Zhang, W. Huang, S. Wu, Catal. Commun. 5 (2004) 729.
[37] B. Mguig, M. Calatayud, C. Minot, J. Mol. Struct. (Theochem.) 709 (2004) 73.
[38] G. Federico, M.N. Marta, G. Antonella, Appl. Catal. B: Environ. 48 (2004) 267–274.
[39] J.M.D. Tascon, L.G. Tejuca, C.H. Rochester, J. Catal. 95 (1985) 558.
[40] X.Y. Jiang, R.X. Zhou, X.X. Yuan, X.M. Zheng, S.S. Jin, Proceedings of the Second Asian Symposium on Academic Activity for Waste Treatment and Resources, 1994, p. 99.
[41] G.A. El-Shobaky, A.I. Ahmed, Sh.El. El-Shafey, Egypt. J. Chem. 52 (6) (2010) 1–23.
[42] B.D. Cullity, Elements of X-ray Diffraction, second ed., Addison-wesely, Publishing Cos., Reading, MA, 1978, p. 102.
[43] G.A. El-Shobaky, S.M. EL-Khouly, A.M. Ghozza, G.M. Mohamed, Appl. Catal. A 302 (2006) 296.
[44] A.M. Ghozza, H.G. El-Shobaky, Mater. Sci. Eng. B 127 (2006) 233.
[45] G.A. El-Shobaky, N.R.E. Radwan, F.M. Radwan, Thermochem. Acta 380 (2001) 27.
[46] Q. Liu, M. Wenping, H. Runxia, M. Zhanjum, Catal. Today 106 (2005) 52–56.
[47] G.A. El-Shobaky, Th. El-Nabarawy, G.A. Fagal, J. Serb. Chem. Soc. 55 (1990) 163.
[48] G.A. El-Shobaky, G.A. Fagal, A.M. Ghozza, M. Mokhtar, Colloids Surf. A: Physicochem. Eng. Aspect 142 (1998) 17.
[49] G.A. El-Shobaky, A.M. Ghozza, H.G. El-Shobaky, Adsorp. Sci. Technol. 16 (1998) 415.
[50] G.A. El-Shobaky, A.N. Al-Noaimi, A.M. Dessouki, Surf. Technol. 26 (1985) 117.
[51] G.A. El-Shobaky, A.N. Al-Noaimi, Bull. Soc. Chim. Fr. 4 (1987) 544.
[52] G. Parravano, Ind. Chem. Eng. 49 (1967) 266.